JEM

Supplemental material

Lauron et al., https://doi.org/10.1084/jem.20181077

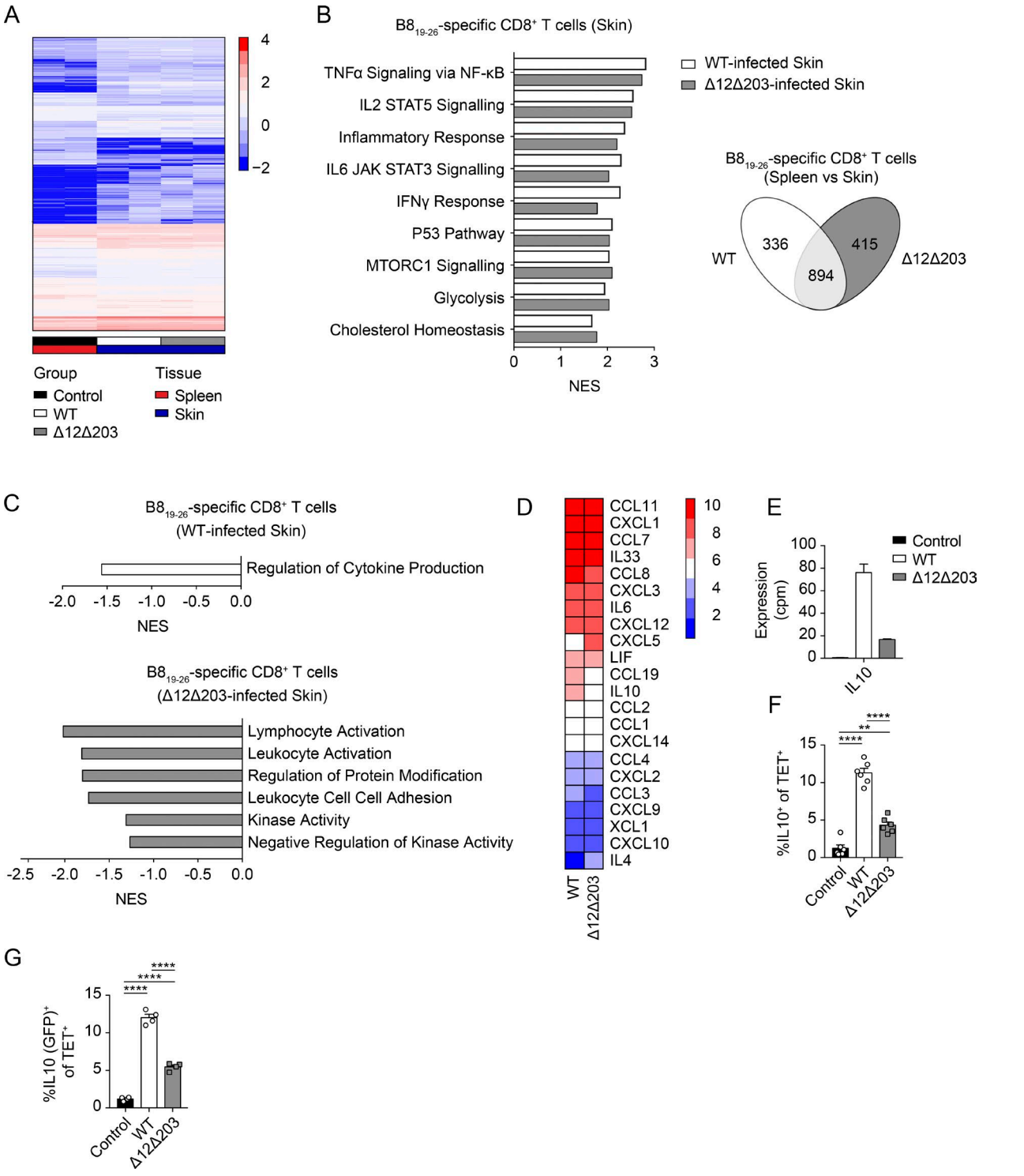

Figure S1. **Skin CD8$^+$ T cells up-regulate local IL-10 production during acute CPXV infection.** C57BL/6 mice were coinfected with WT CPXV and Δ12Δ203 on opposite flanks, and B8$_{19-26}$-tetramer$^+$CD8$^+$ T cells were sorted from the spleen (control) and skin at 7 dpi. **(A)** Heat map showing the genes differentially expressed by B8$_{19-26}$-specific CD8$^+$ T cells from the skin relative to the spleen (adjusted P value cutoff of <0.1 and $\log_2$ fold change > 2). Legend depicts the $\log_{10}$ cpm. **(B)** GSEA profiling of differentially expressed genes (false discovery rate cutoff of <25% and nominal P value of <0.05) and a Venn diagram of genes differentially expressed by B8$_{19-26}$-specific CD8$^+$ T cells in the skin. NES, normalized enrichment score. **(C)** GSEA profiling of differentially expressed genes unique to B8$_{19-26}$-specific CD8$^+$ T cells from WT CPXV– and Δ12Δ203-infected skin. **(D)** Heat map showing the expression of chemokines and cytokines significantly up-regulated by B8$_{19-26}$-specific CD8$^+$ T cells from infected skin. Legend depicts the $\log_2$ fold change. **(E)** IL-10 gene expression by B8$_{19-26}$-specific CD8$^+$ T cells. **(D)** Flow cytometric analyses of IL-10 expression by B8$_{19-26}$-specific CD8$^+$ T cells. Data are pooled from two independent experiments. **(G)** Il10^{GFP} mice were coinfected with WT CPXV and Δ12Δ203 on opposite flanks, and B8$_{19-26}$-specific CD8$^+$ T cells from the spleen and infected skin were analyzed at 7 dpi. Data are pooled from two independent experiments. Symbols represent individual mice. Error bars represent means ± SEM. **, P < 0.01; ****, P < 0.0001; one-way ANOVA followed by Tukey's post-test comparison.

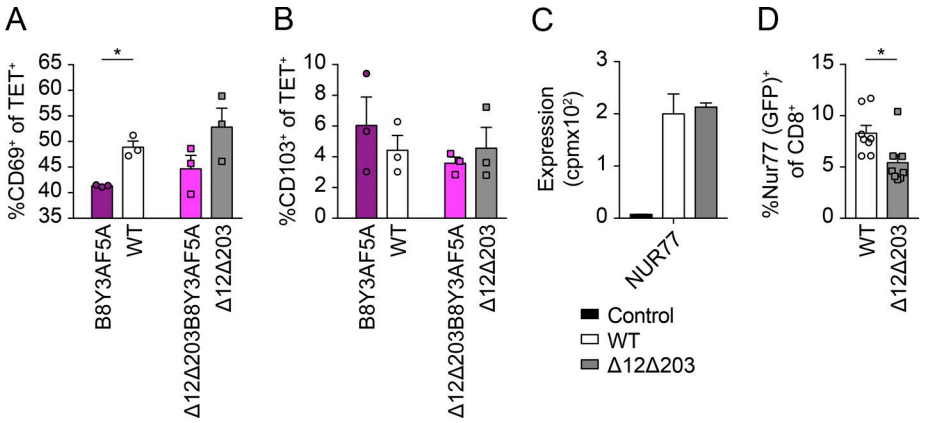

Figure S2. **Local antigen recognition up-regulates CD69 and Nur77 expression by CD8⁺ T cells.** C57BL/6 mice were coinfected by s.s. with $B8_{19–26}$-sufficient (WT or Δ12Δ203) and $B8_{19–26}$-deficient (B8Y3AF5A or Δ12Δ203B8Y3AF5A) CPXV on opposite flanks. **(A)** Percentage of $B8_{19–26}$-tetramer⁺ cells expressing CD69 at 7 dpi. Data are representative of two independent experiments. **(B)** Percentage of $B8_{19–26}$-tetramer⁺ cells expressing CD103 at 7 dpi. Data are representative of two independent experiments. **(C)** Nur77 expression by $B8_{19–26}$-specific CD8⁺ T cells isolated from skin or spleen (control) of coinfected mice at 7 dpi. Data are pooled from two independent experiments. **(D)** $Nur77^{GFP}$ mice were coinfected on opposite flanks with WT CPXV and Δ12Δ203. Nur77 (GFP) expression by CD8⁺ T cells from WT CPXV– or Δ12Δ203-infected skin was analyzed at 7 dpi. Data are pooled from two independent experiments. Symbols represent individual mice. Error bars represent means ± SEM. *, $P < 0.05$; unpaired Student's *t* test.

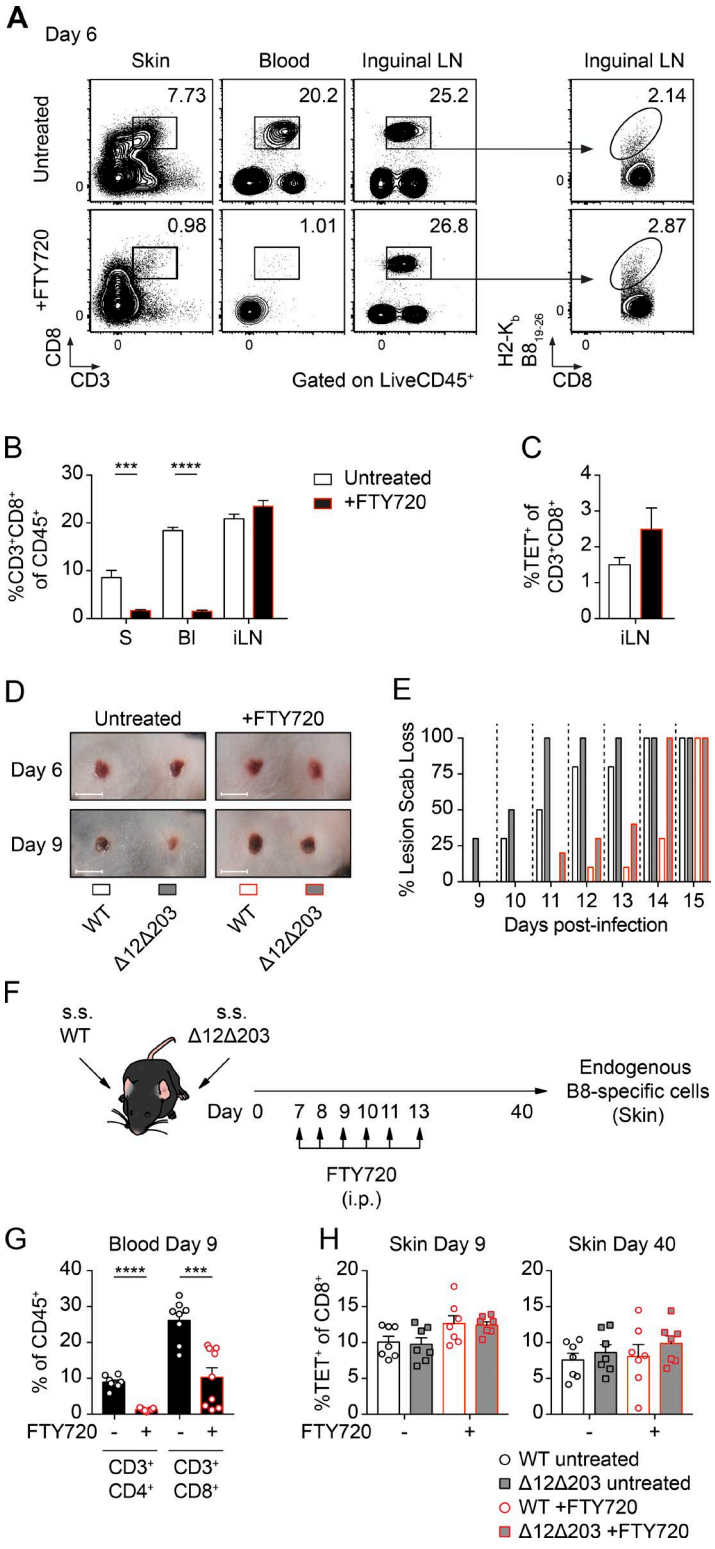

Figure S3. **CD8⁺ T_{RM}s develop without continuous recruitment of CD8⁺ T cells during acute CPXV infection. (A–E)** C57BL/6 mice were coinfected with WT CPXV and Δ12Δ203 on opposite flanks and FTY720 was subsequently administered by i.p injection on 1, 3, and 5 dpi. CD8⁺ T cells were analyzed in the skin (S), blood (Bl), and inguinal lymph node (iLN) at 6 dpi. **(A)** Representative flow plots (n = 9–15 mice per group). Data are representative of two independent experiments. **(B)** Percentage of CD8⁺ cells. Data are pooled from two independent experiments. **(C)** Percentage of $B8_{19–26}$-tetramer⁺ cells in the inguinal lymph node at 6 dpi. Data are pooled from two independent experiments. **(D)** Photographs of skin lesions. Data are representative of two independent experiments (n = 10 mice per group). Bars, 5 cm. **(E)** Lesion scab loss was monitored daily. Data are the combined results from two independent experiments. **(F)** Schematic of coinfection experiment. **(G and H)** T cells from peripheral blood (G) and $B8_{19–26}$-tetramer⁺ cells in the skin (H) of mice infected as shown in F were analyzed at the indicated time points. Data are pooled from two independent experiments. Symbols represent individual mice. Error bars represent means ± SEM. ***, P < 0.001; ****, P < 0.0001; unpaired Student's t test.

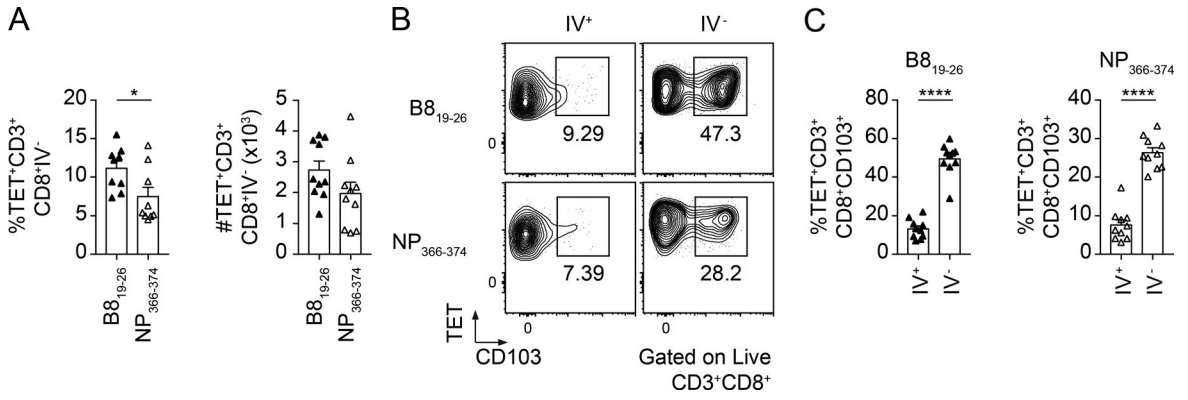

Figure S4. **Flu-B8 respiratory infection generates $B8_{19–26}$-specific $CD8^+$ T_{RM}s in the lungs.** C57BL/6 mice were i.n. infected with recombinant Flu virus expressing the CPXV $B8_{19–26}$ epitope. Intravascular staining with an anti-CD45 antibody was performed before euthanizing mice at 30 dpi. **(A)** Percentage and absolute number of $B8_{19–26}$-tetramer$^+$ and $NP_{366-374}$-tetramer$^+$ IV^- cells in the lungs of Flu-B8–infected mice. **(B)** Representative flow plots of CD103 expression on tetramer$^+IV^-$ cells at 30 dpi. **(C)** Percentage of $CD103^+TET^+IV^-$ cells. Data are pooled from two independent experiments. Symbols represent individual mice. Error bars represent means ± SEM. *, P < 0.05; ****, P < 0.0001; unpaired Student *t* test.

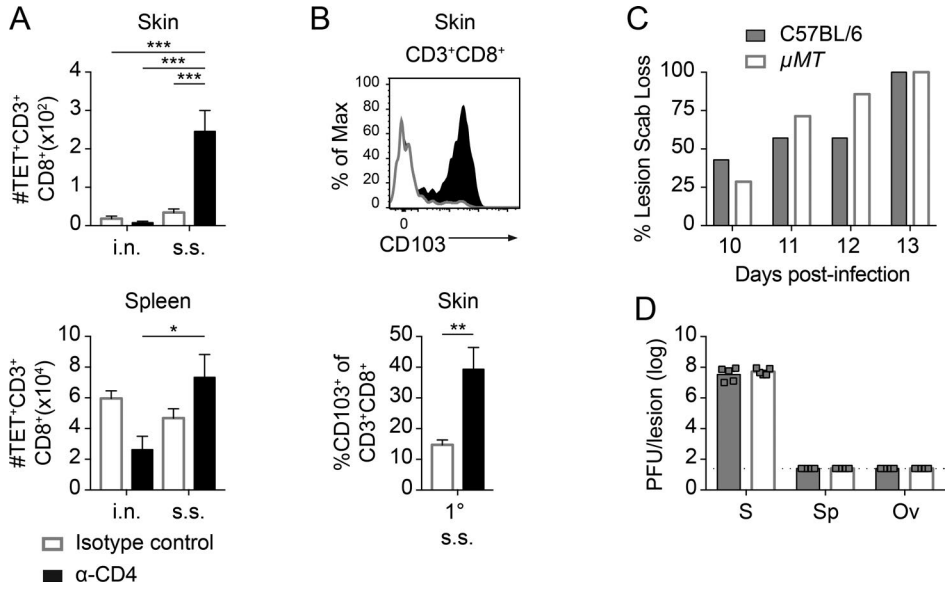

Figure S5. **Number of $CD8^+$ T_{RM}s is reduced in B cell–deficient mice.** μMT mice were infected by s.s. or i.n. with Δ12Δ203 and treated with α-CD4 or isotype control antibodies, as in Fig. 2 D. **(A)** Absolute number of $B8_{19–26}$-tetramer$^+$ cells in the skin and spleen of μMT mice previously infected for 30 d is shown (*n* = 4–5 mice per group). Data are pooled from two independent experiments. **(B)** Representative flow plot of CD103 expression on $CD8^+$ T cells in the skin of μMT previously infected for 30 d is shown above the percentage of $CD103^+$ cells (*n* = 5 mice per group). Data are pooled from two independent experiments. **(C and D)** μMT and C57BL/6 mice were infected by s.s. with Δ12Δ203. **(C)** Infected mice were monitored for lesion scab loss. Data are the combined results from two independent experiments (*n* = 7 mice per group). **(D)** Viral titers were determined from the skin lesions (S), spleens (Sp), and ovaries (Ov) of infected mice at 4 dpi. Data are pooled from two independent experiments. Symbols represent individual mice. Error bars represent means ± SEM. *, P < 0.05; **, P < 0.01; ***, P < 0.001; unpaired Student's *t* test (B and D) or one-way ANOVA followed by Tukey's post-test comparison (A).